
THE UNIVERSITY OF ARIZONA
University Libraries

UA CAMPUS
REPOSITORY

Effect of an environmental flow on vegetation growth and health using ground and remote sensing metrics

Item Type	Article
Authors	Gómez#Sapiens, Martha M.; Jarchow, Christopher J.; Flessa, Karl W.; Shafroth, Patrick B.; Glenn, Edward P.; Nagler, Pamela L.
Citation	Gómez#Sapiens, M. M., Jarchow, C. J., Flessa, K. W., Shafroth, P. B., Glenn, E. P., & Nagler, P. L. (2020). Effect of an environmental flow on vegetation growth and health using ground and remote sensing metrics. Hydrological Processes, 34(8), 1682-1696.
DOI	10.1002/hyp.13689
Publisher	Wiley
Journal	HYDROLOGICAL PROCESSES
Rights	© 2019 John Wiley & Sons Ltd. This article has been contributed to by US Government employees and their work is in the public domain in the USA.
Download date	02/10/2026 23:35:26
Item License	https://creativecommons.org/publicdomain/mark/1.0/
Version	Final published version
Link to Item	http://hdl.handle.net/10150/659868

Check for updates

Received: 20 September 2019 | Accepted: 13 December 2019

DOI: 10.1002/hyp.13689

WILEY

A TRIBUTE TO EDWARD P. GLENN (1947–2017): A LEGACY OF SCIENTIFIC ENVIRONMENTAL ASSESSMENT AND APPLICATIONS IN HYDROLOGICAL PROCESSES

Effect of an environmental flow on vegetation growth and health using ground and remote sensing metrics

Martha M. Gómez-Sapiens[1] | Christopher J. Jarchow[2] | Karl W. Flessa[1] | Patrick B. Shafroth[3] | Edward P. Glenn[4] | Pamela L. Nagler[5]

[1]Department of Geosciences, University of Arizona, Tucson, AZ

[2]Biosystems Engineering, University of Arizona, Tucson, AZ

[3]U.S. Geological Survey, Fort Collins Science Center, Fort Collins, CO

[4]Department of Environmental Science, University of Arizona, Tucson, AZ

[5]U.S. Geological Survey, Southwest Biological Science Center, University of Arizona, Tucson, AZ

Correspondence
Martha M. Gómez-Sapiens, Department of Geosciences, University of Arizona, Tucson, AZ 85721.
Email: gomezsap@email.arizona.edu

Funding information
International Boundary & Water Commission; U.S. Bureau of Reclamation; U.S. Geological Survey; International Boundary and Water Commission; Bureau of Reclamation; Department of Interior; Arizona State University

Abstract

Understanding the effectiveness of environmental flow deliveries along rivers requires monitoring vegetation. Monitoring data are often collected at multiple spatial scales. For riparian vegetation, optical remote sensing methods can estimate growth responses at the riparian corridor scale, and field-based measures can quantify species composition; however, the extent to which these different measures are duplicative or complementary is important to understand when planning monitoring programmes with limited resources. In this study, we analysed riparian vegetation growth in the delta of the Colorado River in response to an experimental pulse flow. Our goal was to compare ground-based measurements of vegetation structure and composition with satellite-based Landsat radiometric variables, such as the normalized difference vegetation index (NDVI). We made this comparison in 21 transects following the delivery of 131.8 million cubic meters (mcm) of water in the stream channel during the spring of 2014 as a pulse flow and 38.4 mcm as base flows. Vegetation cover increased 14% and NDVI increased 0.02 (15%) by October 2015, and both variables returned to pre-pulse flow values in October 2016. Observed changes in vegetation structure and composition did not persist after the second year. The highest increase in vegetation cover in October 2014 and October 2015 resulted from species that could respond rapidly to additional water such as reeds (*Arundo donax* and *Phragmites australis*), cattail (*Typha domingensis*), and herbaceous plants. Dominant shrubs, saltcedar (*Tamarix* spp.) and arrowweed (*Pluchea sericea*), both indicative of nonrestored habitats showed variable increases in cover, and native trees (*Salicaceae* family) presented low increases (1%). The strong NDVI–vegetation cover relationship indicates that NDVI is appropriate to detect changes at the riparian corridor scale but needs to be complemented with ground data to determine the contributions by different species to the observed trends.

KEYWORDS
Colorado River Delta, cover NDVI, environmental flow, riparian monitoring, vegetation structure

This article has been contributed to by US Government employees and their work is in the public domain in the USA.

1 | INTRODUCTION

Riparian systems lie at the interface between aquatic systems and upland communities, supporting high biodiversity and many other ecosystem services (Naiman & Decamps, 1997; Naiman, Decamps, & Pollock, 1993; Poff, Koestner, Neary, & Henderson, 2011; Richardson et al., 2007). The ecological integrity of riparian systems is connected to natural streamflow regime (Poff et al., 1997), and human activities, such as dam and levee construction, channelization, groundwater pumping, and urbanization, have altered the geomorphic and hydrologic dynamics of riparian systems around the world (Carlisle, Wolock, & Meador, 2011; Nilsson & Berggren, 2000; Poff et al., 1997). Thus, the efforts to restore natural flow regimes can conflict with human needs and demands. Environmental flows, defined as "the quantity, quality and timing of water flows necessary to support freshwater and estuarine systems and the ecosystem services that they provide to society" (Acreman et al., 2014), can bridge these potentially conflicting endpoints. In arid and semiarid systems, changes in the frequency and intensity of flooding can alter geomorphologic processes, aquifer recharge, induce intermittency and drought stress on vegetation communities (Nilsson & Berggren, 2000). In turn, the lack of flooding can modify vegetation structure and composition as a result of differences in plants' hydric stress responses (Busch & Smith, 1995). At the landscape level, vegetation expansion or contraction can be correlated to flow dynamics in regulated rivers (Sankey, Ralston, Grams, Schmidt, & Cagney, 2015). Changes in vegetation phenology, the onset of greening and senescence, will shift seasonally and annually according to changes in the contribution of river flow (Jarchow, Nagler, & Glenn, 2017; Jarchow, Nagler, Glenn, Ramírez-Hernández, & Rodríguez-Burgueño, 2017; Nagler, Jarchow, & Glenn, 2018).

Environmental flows need to be coupled with monitoring programmes and protocols designed to understand ecosystem responses, including hydrological, biological, and socio-economic aspects. In particular, the analysis of changes in vegetation structure and composition is often key to understanding the effects of restoration treatments or changes in streamflow (Auble, Friedman, & Scott, 1994; Friedman, Osterkamp, & Lewis, 1996; Stevens et al., 2001). Vegetation monitoring can be undertaken at a range of scales. For example, ground surveys can help to quantify vegetation structure and composition at the local scale (González et al., 2015) and have been used to quantify and model responses of target plant species recruitment, competition, mortality, survival, growth, and water use in relation to flow history or stream hydrologic conditions (Busch & Smith, 1995; Shafroth, Auble, Stromberg, & Patten, 1998; Sprenger, Smith, & Taylor, 2002; Stromberg, 1998).

At the landscape level, remote sensing techniques provide an array of tools to detect changes in land cover types, vegetation health, and vegetation density and to monitor ecosystem processes such as photosynthetic activity, evapotranspiration, and primary productivity across different types of habitats and temporal scales (e.g., Glenn, Huete, Nagler, Hirschboeck, & Brown, 2007; Jarchow et al., 2017; Jensen, 1981; Jones et al., 2008; Pettorelli et al., 2005). The normalized difference vegetation index (NDVI) derived from satellite sensors is one of the most common and applied indices due to its correlation with fractional cover (the cover of green vegetation within a pixel), foliage density, and health or greenness (Carlson & Ripley, 1997; Glenn, Huete, Nagler, & Nelson, 2008; Jiang & Huete, 2010). However, as pointed out by Glenn et al. (2008), these relationships vary across plant communities and require calibration by ground measurements.

In arid and semiarid riparian ecosystems, NDVI has been used to evaluate the vegetation response to stream flows (Jarchow et al., 2017; Jones et al., 2008; Nagler, Glenn, & Huete, 2001; Nguyen, Glenn, Nagler, & Scott, 2015; Zhao, Wei, Li, & Wu, 2016). Moreover, in these systems, NDVI is positively correlated to fractional cover (Nagler et al., 2001; Nagler, Glenn, Thompson, & Huete, 2004). This allows monitoring vegetation trends at a riparian corridor scale. However, integrating ground data can lead to a better interpretation of responses in NDVI trends. In particular, analysis of vegetation response to flows at different spatial scales is required in order to understand what groups of species are benefiting from flows and facilitate the scaling process from field-based metrics to metrics retrieved using remote sensing methods (Glenn, Nagler, & Huete, 2014).

In the Colorado River, the construction of major dams between the 1930s and 1960s resulted in significant alteration to the natural flow regime, reducing the average daily discharge by ~37% (Mueller et al., 2017). The Minute 319 agreement between the United States and Mexico allowed the delivery of the first environmental flows into the section of the Colorado River along the Mexico–U.S. border and lower reaches towards the river's delta (International Boundary and Water Commission, 2012). In the spring of 2014, a volume of 130 million cubic meters (mcm) was delivered as a pulse flow from the United States to the stream channel in Mexico (Pitt & Kendy, 2017; Ramírez-Hernández, Rodríguez-Burgueño, Kendy, Salcedo-Peredia, & Lomelí, 2017), and an additional 56.5 mcm was provided as base flows from 2014 to 2016 (International Boundary and Water Commission, 2018). The aim of this experimental flow was to enhance bird riparian habitats by promoting the recruitment of native cottonwoods (*Populus fremontii*) and willows (*Salix gooddingii*).

In the years following Minute 319, a team of scientists analysed the biological and hydrological response to the pulse (see Ecological Engineering, Special Issue, Vol. 106 Part B edited by Glenn et al., 2017, on the Delta Environmental Flows). The results from these studies showed an increase of 17% in vegetation greenness based on NDVI following the pulse in 2014 (Jarchow et al., 2017) and minimal recruitment of riparian mesic species (*P. fremontii* and *S. gooddingii*) outside of active restoration areas (Shafroth et al., 2017).

In this study, we compare ground-based measurements of vegetation structure and composition to satellite-based NDVI from Landsat following the Minute 319 pulse flow. Our specific objectives were to (a) analyse community composition, structure, and greenness through NDVI changes after the 2014 pulse flow and (b) determine what groups of species contributed in a higher degree to changes in NDVI or greening up responses.

2 | METHODS

2.1 | Study sites

The study sites in the Lower Colorado River were distributed along 90 km of river beginning at the U.S.–Mexico border between Morelos Dam at the Northern International Boundary and extending towards the Gulf of California (Colorado River Delta sites; Figure 1). The study area has a range of mean annual temperatures of 21.9°C to 23.7°C, mean maximum temperature on July of 38.8°C to 43.3°C, and mean annual precipitation of 60.4 mm (Yuma Valley station, 1995–2015, The Arizona Meteorological Network, http://ag.arizona.edu/azmet/).

2.1.1 | Streamflow in the riparian corridor

River flows in the Colorado River Delta have progressively decreased as a result of water diversion and construction of dams upstream. In years previous to the presence of the dams, from 1905 to 1936, peak flows could exceed 5,000 m^3/s, and daily discharges averaged 600 m^3/s; however, by the early 1960s, peak flows were reduced to 581 m^3/s, and the daily discharge averaged 93 m^3/s (Figure 2; Mueller et al., 2017).

In subsequent years, flows into the Colorado River Delta were reduced to almost zero, until 1983–1987 and the years 1993, 1997, 1999, and 2000 when runoff exceeded storage capacity in the watershed and daily discharge peaks ranged from 100 to above 934 m^3/s, promoting the recruitment of native cottonwoods and willows (Cohen, Henges-Jeck, & Castillo-Moreno, 2001; Mueller et al., 2017; Zamora-Arroyo & Nagler et al., 2001). After 2000, a drought period started in the watershed again reducing the flows in the Colorado River Delta to almost zero with occasional spills with peaks of less than 200 m^3/s (Hinojosa-Huerta, Nagler, Carrillo-Guerrero, & Glenn, 2013).

The 2014 pulse flow, which occurred from March to May, delivered a total of 131.9 mcm from three main delivery points (Figure 2),

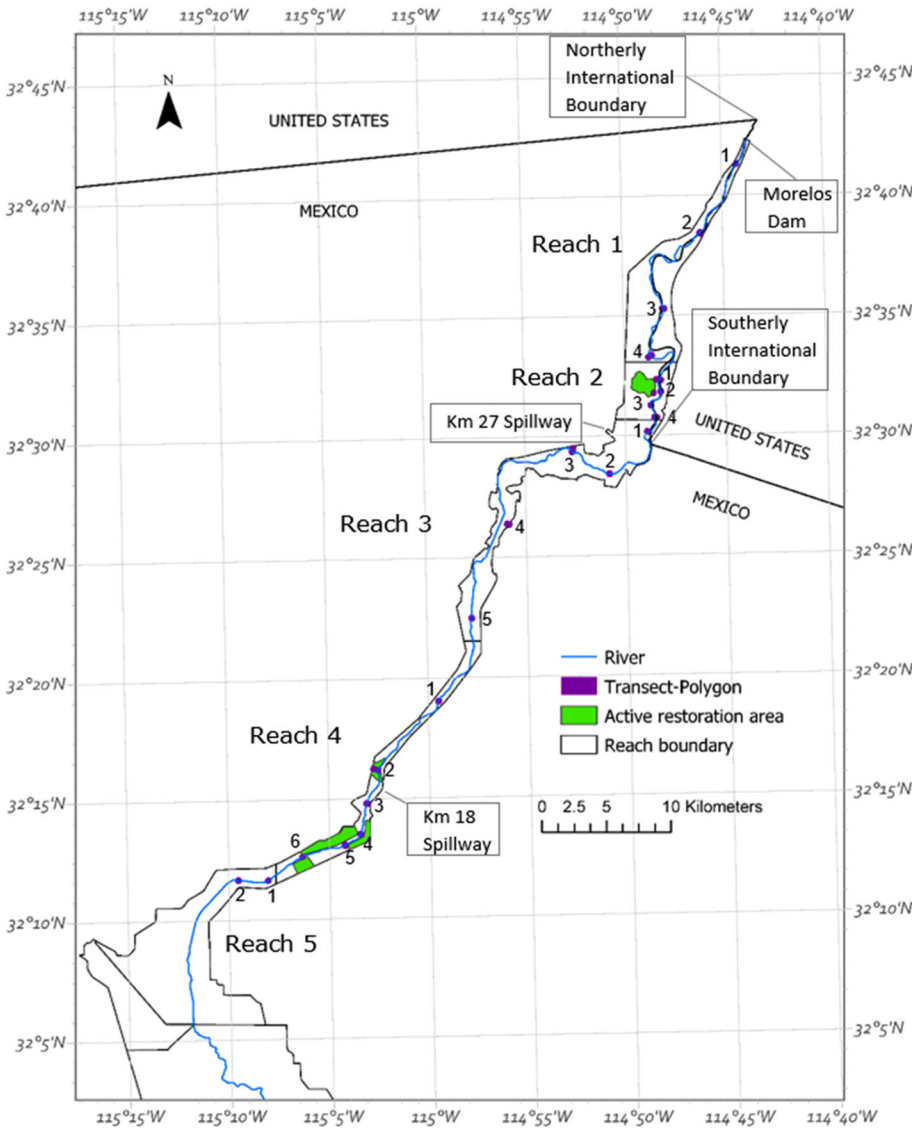


FIGURE 1 Location of transects and normalized difference vegetation index polygons in the Colorado River Delta riparian corridor

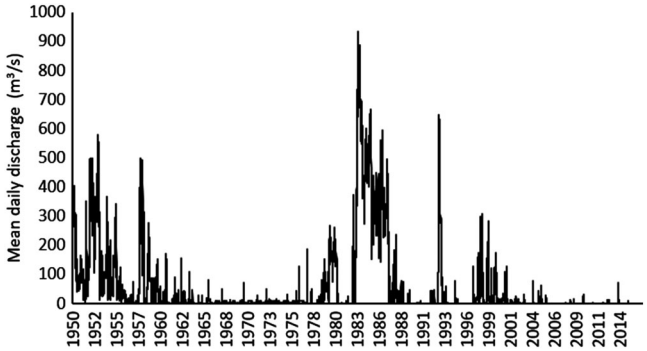


FIGURE 2 Mean daily discharge (m^3/s) at the Southerly International Border, at the San Luis Rio Colorado Bridge, located 21 miles below the Morelos dam. Data from International Boundary Water Commission, U.S. Section

101.7 mcm was delivered through Morelos Dam with a peak discharge of 119 m^3/s, 20.9 mcm was delivered through the km 27 spillway with a peak discharge of 23.8 m^3/s, and 9.3 mcm was delivered through the km 18 spillway, with a peak discharge of 9.7 m^3/s (Ramírez-Hernández et al., 2017; Shafroth et al., 2017). Additional low flows from Morelos Dam were delivered from September 5 to September 10, 2014, and had a total volume of 5.1 mcm, and from May 18 to the end of October 6, 2014, 7 mcm was delivered from km 18 spillway as base flows (Shafroth et al., 2017).

In 2015, from May 16 to May 19, a volume of 28.2 mcm with a peak flow rate of 235 m^3/s was delivered through Morelos Dam; this flow inundated Reaches 1 and 2. During the 2015 and 2016 growing seasons, low flows were delivered in Reach 2 and Reach 4 using irrigation infrastructure to support target restoration sites (Miguel Aleman and Laguna Grande, Figure 2). Low flows had a volume of 1.4 and 0.8 mcm in 2015 and 2016, respectively, in restoration site Miguel Aleman located in Reach 2 (International Boundary and Water Commission, 2018). In Reach 4, deliveries had a volume of 10.7 mcm in 2015 and 15.5 mcm in 2016 (International Boundary and Water Commission, 2018).

2.1.2 | Environmental conditions by reach

The reach boundaries were based on previous characterizations of hydrological and biological conditions (Flessa et al., 2013). Vegetation communities are dominated by an introduced shrub, saltcedar (*Tamarix* spp.), with 10% or less of these communities containing native trees, cottonwoods (*P. fremontii*), and willow (*S. gooddingii*).

Reach 1 begins at Morelos Dam, where the river's water is diverted to the Mexicali Valley Irrigation District. In this reach, groundwater elevation in the channel is above the channel elevation, due seepage from the dam and irrigation (Kennedy, Rodríguez-Burgeño, & Ramírez-Hernández, 2017; Ramírez-Hernández, Hinojosa-Huerta, Peregrina-Llanes, Calvo-Fonseca, & Carrera-Villa, 2013). During the course of this study, we observed variation in the extent of the surface water downstream of Morelos Dam. The plant communities are composed of the non-native shrub *Tamarix* spp. and low proportions of mesic native trees *P. fremontii* and *S. gooddingii* as well as shrubs *Baccharis* spp. (seep willow and willow baccharis) and the facultative wetland shrub *Pluchea sericea* (arrowweed; Nagler et al., 2005; Zamora-Arroyo & Nagler et al., 2001). The riverbed is generally dominated by dense stands of *Arundo donax* (giant reed) and *Phragmites australis* (common reed) with some patches of wetland obligate species *Typha* spp. (cattail) and *Schoenoplectus* spp. (bulrush).

Reach 2 extends from river km 20–31 and has deeper groundwater, reaching almost 10 m in some sections (Kennedy et al., 2017). Along this reach, the streambed is dry and transitions into a wider and sandier channel, similar to that in Reach 3 (below). Native trees are sparse, and most of the vegetation is composed of *Tamarix* spp., *P. sericea* and *Prosopis* spp. (Mesquite).

Reach 3 starts a few km upstream the Southern International Boundary at river km 31 and ends at river km 60. In this reach, groundwater depth can exceed 10 m due a cone of depression or zone where the groundwater level drops due groundwater pumping (Kennedy et al., 2017). The proportion of *Tamarix* spp. in relation to other species as *P. sericea* is the highest in this reach (Nagler et al., 2005).

Reach 4 extends from river km 60 to river km 86. This reach has perennial water as a result of irrigation return flows, and the groundwater level is similar to the channel elevation (Kennedy et al., 2017; Ramírez-Hernández, Rodriguez-Burgueño, Zamora-Arroyo, Carreon-Diazconti, & Perez-Gonzalez, 2015). Groundwater depth and surface water vary with the irrigation season, and water level raises from March to June during the high irrigation months and lowers from August to January during low irrigation (Ramírez-Hernández et al., 2015). These hydrologic conditions support a resurgence of mesic species in the floodplain including *P. fremontii*, *Salix* spp., and *Baccharis* spp., dense stands of *Tamarix* spp., *P. sericea*, and *Atriplex* spp., and emergent species *A. donax*, *P. australis*, *Schonoeplectus* spp., and *Typha* spp. in the stiff river banks (Hinojosa-Huerta et al., 2013; Nagler et al., 2005).

Reach 5 extends from river km 90 to river km 105. The upper part of this reach is dry, but the groundwater level is high and supports native trees and riparian shrubs (e.g., *Baccharis* spp.). Emergent vegetation resurges during wet periods in some portions of the channel. The lower part of this reach has surface water and marshland vegetation.

2.2 | Ground vegetation surveys

We estimated the percentage of live vegetation cover, by species, along 21 transects distributed in the riparian corridor from Reach 1 to the upper portion of Reach 5 along 93 km of the river (Figure 1). We installed rebar at the ends of each transect and at some intermediate points so that we could resurvey the same locations throughout the study period. Transects were oriented perpendicular to the river channel and included the area inundated by the 2014 pulse flow. Along five of the transects, a separate section was added across side

channels that were inundated in 2014. Transect length varied from 70 to 450 m depending on the inundation extent.

We conducted vegetation surveys after the pulse flow at the end of the growing seasons in October 2014, 2015, and 2016. In sites where the transect length was modified in subsequent years, we adjusted the length to compare cover on the same portion of the transect across years.

We used a line intercept method (Canfield, 1941) to record the cover of trees, shrubs, herbaceous, open water, and bare ground, while excluding cover of new seedlings because it was minimal, and in most cases, these were grouped with herbaceous cover. Absolute per cent of cover was calculated by transect for each species or group of species as the per cent of transect occupied by that cover type. We grouped *Baccharis salicifolia* and *Baccharis salicina* as BASP, herbaceous species were grouped as HERBS, *A. donax* and *P. australis* were grouped as ARDO-PHAU, *Atriplex* spp. as ATSP, and *Tamarix* spp. as TASP. Vegetation cover per transect was calculated summarizing the absolute per cent of cover of species/groups.

2.3 | NDVI estimations

We selected four cloud-free Landsat 8 Operational Land Imager (OLI) scenes. The selected 30-m spatial resolution images were composed of surface reflectance and the corresponding NDVI data for each year in the period 2013–2016. Only data from the growing season (May to October) were acquired from the Earth Resources Observation Science Center Science Processing Architecture (see Table 1 for scene information). Images are atmospherically corrected surface reflectance, and the derived NDVI is based on the L8SR algorithm (Vermote et al., 2016) following

$$(NIR - R)/(NIR + R), \quad (1)$$

where *NIR* is reflectance in the near infrared band (OLI Band 5) and *R* is reflectance in the red band (OLI Band 4). Following Groeneveld and Baugh (2007), we scaled (stretched) NDVI values between bare soil and maximum vegetation for each respective scene, thereby eliminating nonsystematic variation between scenes (see Jarchow et al., 2017, for a complete description of this process). Scaled NDVI (*NDVI**) is calculated as

$$NDVI^* = (NDVI - NDVI_0)/(NDVI_s - NDVI_0), \quad (2)$$

where $NDVI_0$ is NDVI of bare soil and $NDVI_s$ is NDVI at full vegetation cover (saturation). We calculated $NDVI_0$ and $NDVI_s$ for each reach and year and calculated mean growing season *NDVI** for each year.

We applied a 60-m buffer to each transect line using ArcGIS (v. 10.4, ESRI, Inc., Redlands, CA) and extracted mean NDVI* from each buffered transect using Zonal Statistics. The buffering addresses geolocation error (Storey et al. 2016) in the 30-m OLI data and guarantees that the line transect would reside within the buffer extent. In cases where buffered transects overlapped, we took the average of the overlapping transects.

TABLE 1 Scene acquisition period, path, and rows for all Landsat 8 Operational Land Imager included in the normalized difference vegetation index analysis

Acquisition dates	Path	Rows
May 24, 2013	38	37/38
June 25, 2013	38	37/38
August 12, 2013	38	37/38
October 31, 2013	38	37/38
May 27, 2014	38	37/38
June 28, 2014	38	37/38
August 31, 2014	38	37/38
October 2, 2014	38	37/38
May 30, 2015	38	37/38
June 15, 2015	38	37/38
August 18, 2015	38	37/38
October 21, 2015	38	37/38
May 16, 2016	38	37/38
June 17, 2016	38	37/38
September 5, 2016	38	37/38
October 23, 2016	38	37/38

2.4 | Statistical analysis

To determine if vegetation cover and NDVI* changed after the pulse flow, we conducted a one-way repeated measures analysis of variance (ANOVA) on NDVI* growing season mean and vegetation cover as measured along the transects. We treated the values from transects as repeated measurements and year as the repeated factor. We used post hoc tests with Bonferroni correction (Bland & Altman, 1995) to determine in which years differences in vegetation cover and NDVI* occurred. Data were transformed to natural log (ln) to meet normality assumptions.

To determine the relationship between vegetation cover and NDVI*, we performed a simple linear regression on NDVI* in SPSS (version 24; IBM Corp., 2016) for each year and compared the equation's regression coefficients. We verified random distribution of residuals in the three data sets to meet linear regression model assumptions.

To quantify differences in community structure, we used a Bray–Curtis dissimilarity index (Bray & Curtis, 1957) comparing pair of years (2014 vs. 2015 and 2015 vs. 2016) using the equation

$$\sum_{j=1}^{J} \frac{|nij - ni'j|}{ni + ni'}, \quad (3)$$

where *nij* represents the per cent cover of each species in Sample 1 and $ni'j$ in Sample 2, *ni* is the sum of covers of all species in Sample 1, and ni' is the sum of covers of all species from the sample (Ricotta and

Podani, 2017). The index ranges from 0 to 1, and a value of 0 indicates identical community structure between samples; therefore, dissimilarity increases as values get close to 1.

To assess changes in community composition, we considered plant assemblages based on per cent cover, including only species or group of species with per cent cover ≥5% on each transect. Transect 2-1 had per cent of cover <5% by species or group of species during 2014 and 2016; therefore, we used the maximum value by species or combined by group of species.

To evaluate species contributions to changes in vegetation cover and ultimately NDVI* from 2014 to 2016, we determined the species/groups that had changes in cover from one growing season to another, by transect. We compared the increases or decreases (per cent difference) in vegetation cover with increases or decreases in NDVI by transect.

3 | RESULTS

3.1 | Vegetation cover and NDVI* after the 2014 pulse flow

Mean vegetation cover and mean NDVI* in the riparian corridor followed similar, but not equal, trends during sampling years (Figure 3). Vegetation cover in transects showed the highest increase during the second growing season following the pulse flow (2015), whereas NDVI* increased during the growing season in the year of the pulse flow (2014).

Mean vegetation cover increased in the riparian corridor transects after the pulse flow year from 33.1% (*SD* = ±22.7) to 47.2% (*SD* = ±37.9) in 2015 and then decreased to 34.9% (*SD* = ±25.5) in 2016, $F(2, 40) = 15.80$, $p < .001$, from repeated measures ANOVA. Post hoc tests indicate the differences occurred between the first and second years ($p < .001$) and between the second and third years ($p = .002$). We did not find differences between the first and third years ($p = 1$).

Mean NDVI* from transects (Figure 3) increased from 0.20 (*SD* = ±0.12) in 2013 to 0.23 (*SD* = ±0.12) in 2014, remained unchanged in 2015 (*SD* = ±0.13), and returned to 0.20 (*SD* = ±0.14) in 2016, $F(3, 60) = 16.02$, $p = <.001$, from repeated measures ANOVA. Post hoc tests confirmed significant differences resulted from pairwise comparisons between 2013 versus 2014 ($p = .003$), 2013 versus 2015 ($p = .026$), 2014 versus 2016 ($p = .002$), and 2015 versus 2016 ($p = .003$).

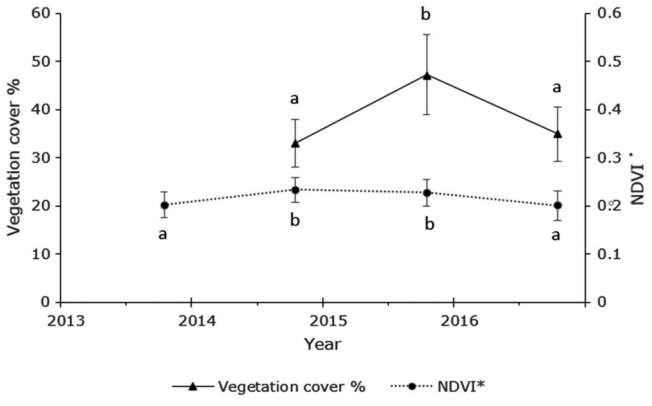


FIGURE 3 Mean vegetation cover along field transects (triangles) and growing season NDVI* from Landsat images (circles). Error bars are the standard error of the mean from 21 transects in the riparian corridor. Different letters indicate significant differences between years ($p < .05$) from post hoc tests. NDVI, normalized difference vegetation index

3.2 | Vegetation cover and NDVI* relationships from transects

NDVI* was strongly correlated with vegetation cover in each year ($p < .001$, $R^2_{2014} = .84$; $R^2_{2015} = .87$; $R^2_{2016} = .88$) along the riparian corridor (Figure 4). Years 2014 and 2016 had very similar regression coefficients (174.9 and 172.8, respectively). In contrast, the regression coefficient of the 2015 relationship was the highest (264.0) due to high cover values associated with high NDVI* values in transects from Reaches 1, 4, and 5 where cover increased 60–90% from 2014 to 2015.

3.3 | Changes in community composition, structure, and NDVI* by transect

From 2014 to 2015, the perennial transects in Reach 1 showed changes in community composition (Table 2). Vegetation cover increased 41% and 31% in Transects 1-2 and 1-3, respectively, but remained unchanged in Transect 1-1 (Figure 5). Species that showed the highest increases in cover in the three transects included *P. sericea*, non-native reeds *A. donax* and *P. australis*, *Tamarix* spp., and to a lesser degree native trees Goodding's willow (*S. gooddingii*) and Fremont

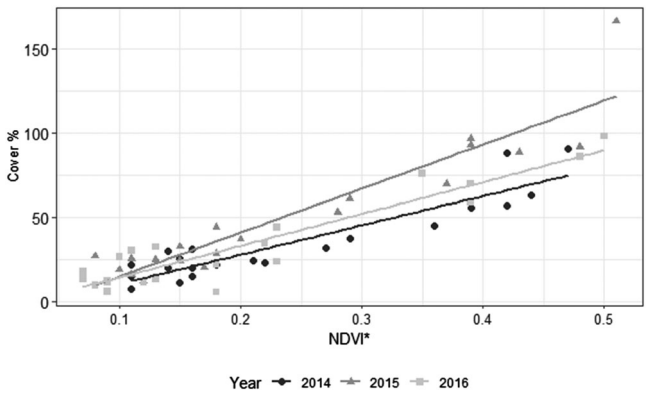


FIGURE 4 Regression lines from scaled NDVI (NDVI*) in 60-m buffer polygons created around the 21 vegetation transects and vegetation cover along the transects. NDVI, normalized difference vegetation index

TABLE 2 Plant assemblage showing the species with the highest contribution in per cent cover using a threshold of 5% cover

Transect	2014	2015	2016
1-1	ARDO-PHAU (40.9)	TASP (30.8)	ARDO-PHAU (36.4)
	TASP (24.6)	ARDO-PHAU (26.4)	PLSE (26.2)
	PLSE (15.5)	PLSE (22.7)	TASP (25.2)
	SAGO (7.5)	SAGO (9.0)	SAGO (10.4)
1-2	PLSE (17.1)	PLSE (30.2)	PLSE (19.3)
	HERBS (9.9)	ARDO-PHAU (12.5)	ARDO-PHAU (10.7)
	BASP (7.6)	TASP (10.8)	TASP (6.8)
	TASP (6.0)	SCAM (10.5)	SAGO (6.7)
	SAGO (5.9)	HERBS (10.5)	POFR (5.0)
		SAGO (7.8)	
		BASP (7.2)	
		POFR (5.9)	
1-3	ARDO-PHAU (10.9)	ARDO-PHAU (18.5)	TASP (10.6)
	TASP (8.8)	TASP (14.4)	
		HERBS (10.0)	
		PLSE (8.8)	
1-4	TASP (21.1)	TASP (22.5)	TASP (15.8)
2-1	TASP (4.9)	TASP (9.2)	TASP (3.8)
2-2	TASP (10.0)	TASP (12.6)	TASP (11.6)
2-3	TASP (23.1)	TASP (29.1)	TASP (25.3)
		PLSE (11.8)	PLSE (6.9)
2-4	TASP (18.1)	TASP (27.2)	TASP (21.9)
3-1	TASP (12.8)	TASP (16.6)	TASP (14.1)
3-2	TASP (10.2)	TASP (10.3)	TASP (11.5)
3-3	TASP (16.4)	TASP (18.2)	TASP (12.5)
3-4	TASP (21.4)	TASP (24.9)	TASP (22.4)
3-5	TASP (24.9)	TASP (24.3)	TASP (23.7)
4-1	TASP (14.1)	TASP (11.9)	TASP (18.8)
		PLSE (7.1)	
		ARDO-PHAU (6.1)	
4-2	PLSE (15.8)	ARDO-PHAU (29.4)	TYDO (5.9)
	ARDO-PHAU (14.9)	PLSE (18.0)	
	TASP (11.7)	TASP (11.5)	
	BASP (10.2)	HERBS (9.4)	
		BASP (6.4)	
4-3	TASP (9.9)	TASP (12.9)	PLSE (14.5)
	ARDO-PHAU (9.2)	PLSE (12.7)	TASP (10.6)
	PLSE (9.0)	ARDO-PHAU (12.7)	ARDO-PHAU (10.4)
	ATSP (8.2)	ATSP (11.8)	ATSP (7.5)
4-4	TASP (10.4)	TASP (14.9)	TASP (15.2)
	PLSE (6.6)	PLSE (10.1)	PLSE (12.9)
		TYDO (9.1)	
4-5	PLSE (11.3)	TYDO (19.7)	TYDO (19.9)
	TYDO (9.0)	PLSE (18.5)	PLSE (16.0)
	TASP (8.8)	TASP (13.9)	TASP (10.4)
	BASP (6.2)	ARDO-PHAU (6.1)	BASP (5.0)
		BASP (5.5)	

(Continues)

TABLE 2 (Continued)

Transect	2014	2015	2016
4-6	TYDO (26.9)	TYDO (53.7)	TYDO (27.1)
	PRPU (18.9)	HERBS (33.9)	TASP (19.4)
	TASP (16.0)	TASP (24.8)	PLSE (13.6)
	HERBS (10.2)	PLSE (17.2)	PRPU (10.5)
	BASP (5.7)	PRPU (14.3)	BASP (9.0)
	SAGO (5.0)	BASP (10.2)	SAGO (6.8)
		SAGO (6.9)	
5-1	TASP (34.9)	TASP (53.5)	PLSE (32.9)
	PLSE (18.0)	PLSE (31.6)	TASP (29.9)
		BASP (7.6)	BASP (5.0)
5–2	TASP (21.0)	TASP (19.7)	TASP (17.1)
	PLSE (6.7)		PLSE (13.4)

Notes: Per cent cover values are in parenthesis. Species codes are ARDO-PHAU, *Arundo donax* + *Phragmites australis* (reeds); ATSP, Atriplex spp. (quailbush); BASP, *Baccharis spp*., HERBS, mixed herbaceous; PRPU, *Prosopis pubescens* (screwbean mesquite); PLSE, *Pluchea sericea* (arrowweed); POFR, *Populus fremontii* (cottonwood); SAGO, *Salix gooddingii* (gooddingii's willow); SCAM, *Schoenoplectus americanus* (bulrush); TASP, *Tamarix spp*. (saltcedar); TYDO, *Typha domingensis* (cattail).

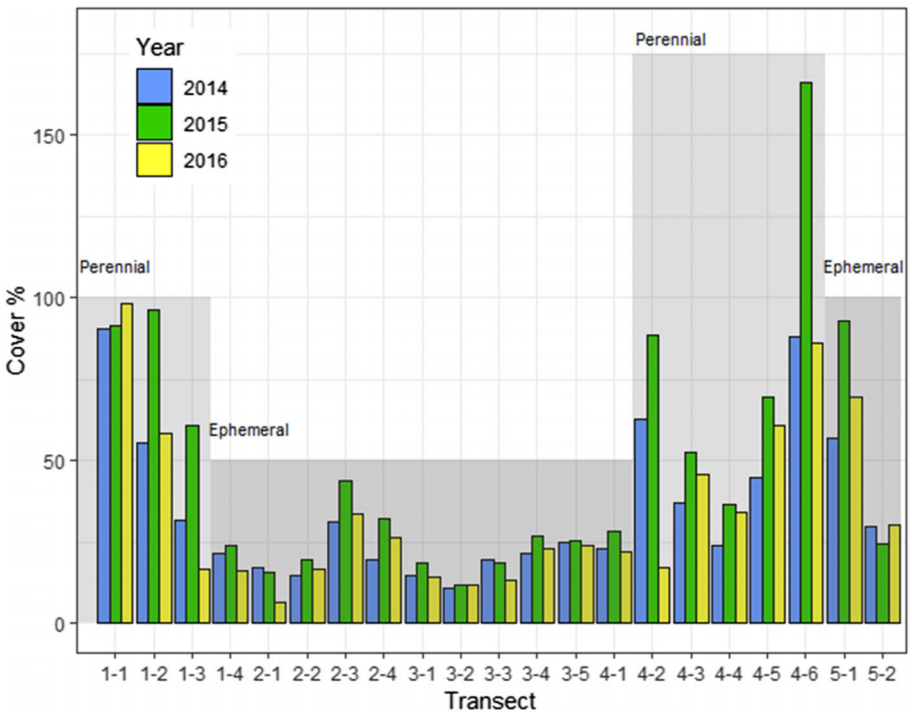


FIGURE 5 Vegetation cover along 21 transects in after the growing season of years 2014, 2015, and 2016

cottonwood (*P. fremontii*). Vegetation structure changes quantified using the dissimilarity index showed values that ranged from 0.19 to 0.35 (Figure 6). On the other hand, NDVI* did not show responses to change in cover, showing very similar values from 2014 to 2015 (0.47 and 0.48 in Transect 1-1, 0.39 in Transect 1-2, and 0.27 and 0.29 in Transect 1-3; Figure 7).

From 2015 to 2016, vegetation cover in Transect 1-1 increased but decreased in Transects 1-2 and 1-3 by about 40% (Figure 5). Community composition and structure (see Table 2 and Figure 6) remained the same in Transect 1-1, but in the two other transects, the number of species with cover ≥5% was lower, and dissimilarity indices varied from 0.26 to 0.57. NDVI* showed almost no change in Transect 1-1, but decreased in the next two transects: from 0.39 to 0.35 in Transect 1-2 and from 0.29 to 0.18 in Transect 1-3 (Figure 7).

In the transects where the river becomes ephemeral (Transect 1-4 and all transects in Reaches 2 and 3), vegetation cover showed small increases or no change from 2014 to 2015 (Figure 5).

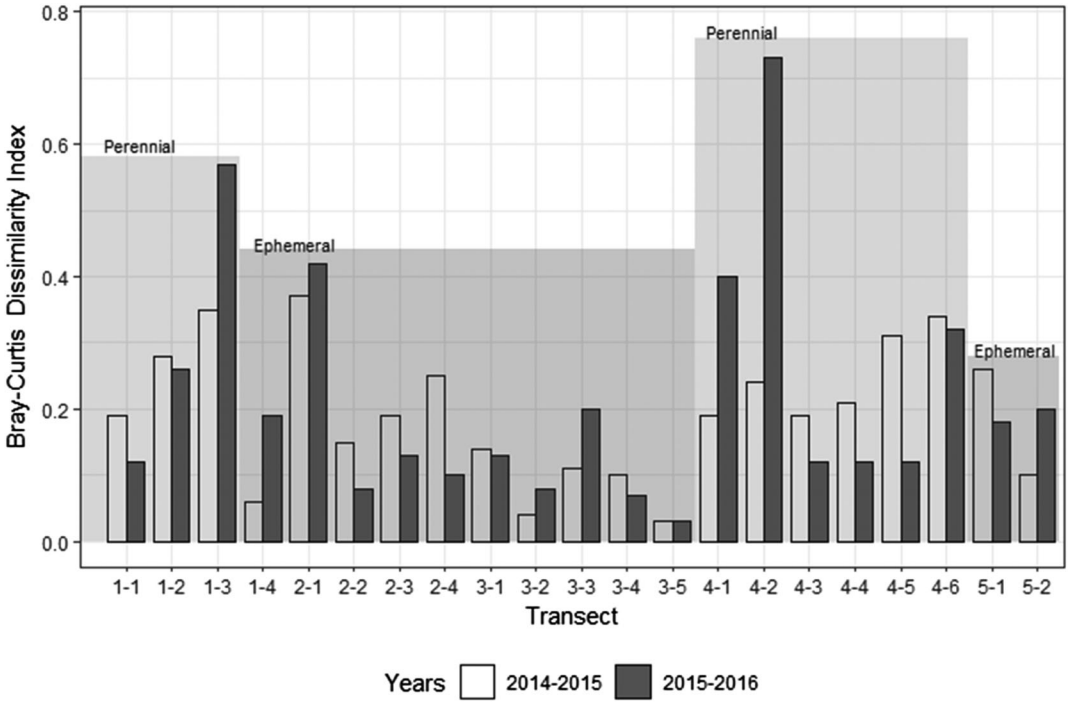


FIGURE 6 Bray–Curtis dissimilarity index based on species cover value in pair of years 2014–2015 and 2015–2016

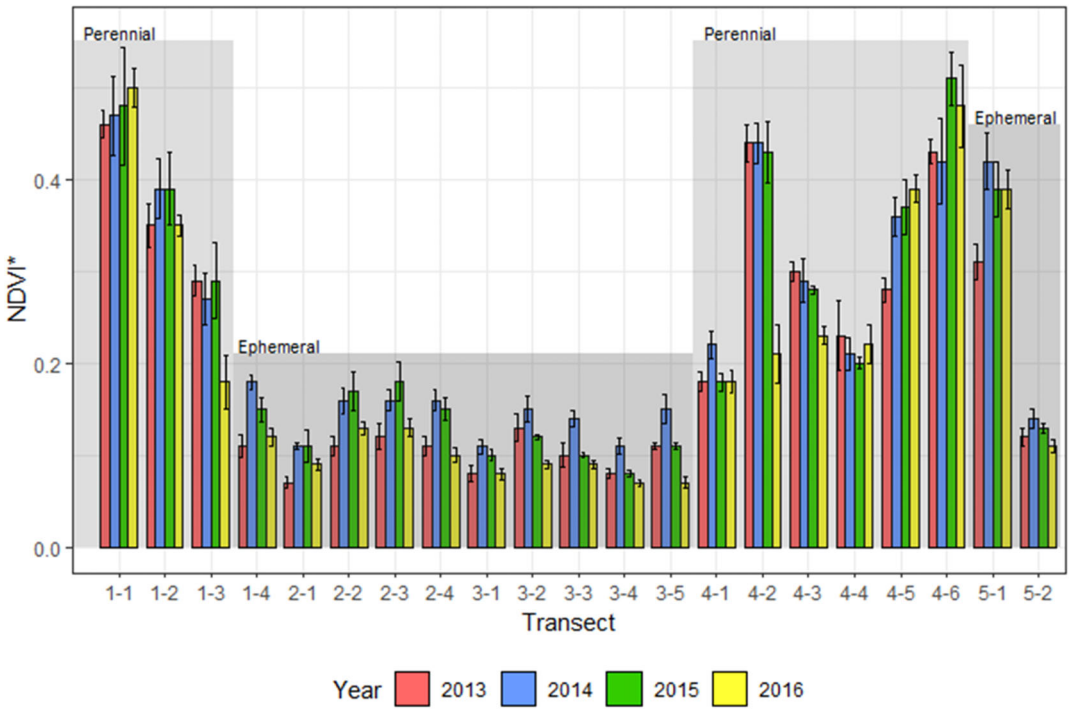


FIGURE 7 Mean NDVI* and standard error, in 21 transects measured in Landsat scenes from May, June, August or September, and October before the pulse flow (2013) and after (2014, 2015, and 2016). NDVI, normalized difference vegetation index

Maximum increases in vegetation cover were around 12%. Dissimilarity index values ranged from 0.03 to 0.37, with most of the values below 0.20 (Figure 6). Increases in the dominant species, *Tamarix* spp., varied from 0.1% to 9.1% cover (Table 2). Major increases in NDVI* occurred during the pulse flow year (2014) compared with the previous year from 2014 to 2015 NDVI* remained the same or showed small decreases (≤0.04) in Transect 1-4 and all transects in Reach 3 (Figure 7).

From 2015 to 2016, vegetation cover in the ephemeral portions of the riparian corridor showed decreases in the range of 0.4–10% (Figure 5). *Tamarix* spp. cover values ranged from 1% to 6.7% (Table 2). Dissimilarity index values ranged from 0.03 to 0.42, with most values around 0.1 (Figure 6). Decreases in NDVI* ranged from 0.01 to 0.05, within the upper boundary of VI error in sparsely vegetated areas, and these decreases did not always correlate with changes in cover (Figures 5 and 7).

In the perennial transects from Reach 4 and ephemeral transects from Reach 5, the highest increases in vegetation cover were observed between 2014 and 2015. Increases ranged from 10% to 78%, with the exception of transects at the start and end of this section of the riparian corridor (4-1 and 5-2) where vegetation cover increased or decreased about 5%, respectively (Figure 5). The species that contributed to the increases varied by transect (Table 2). In Transect 4-2, *A. donax–P. australis* group and herbaceous species contributed the most to increases in cover. In Transects 4-3 and 4-4, most of the species contributed equally to the increases. In transects with the highest increases from 2014 to 2015 (4-5 and 4-6), *Typha domingensis*, herbaceous species, *P. sericea*, and *Tamarix* spp. showed the greatest increases in cover. Dissimilarity index had a range of 0.10 to 0.34, with highest values in Transects 4-5 and 4-6 (Figure 6). NDVI* showed an increase from 2013 to 2014 in Transects 4-1, 4-5, and both transects of Reach 5, indicating a pulse flow effect. NDVI* values remained the same from 2014 to 2015 in all transects with exception of 4-1 where NDVI* decreased and 4-6 where NDVI* increased (Figure 7).

From 2015 to 2016, vegetation cover decreased from 2% to 80% in all the transects in Reach 4 and Transect 5-1 from Reach 5 (Figure 5). These decreases corresponded to a decrease in cover of *P. sericea* and the *A. donax–P. australis* group in Transect 4-1, almost all the species in Transects 4-2 and 4-3, reductions in the cover of *T. domingensis* in Transect 4-4, *A. donax–P. australis* group in Transect 4-5, herbaceous species, *T. domingensis* and *Tamarix* spp. reductions in Transect 4-6, and a significant decrease in the cover of *Tamarix* spp. in Transect 5-1 (Table 2). Dissimilarity index values ranged from 0.12 to 0.73, with the highest values of 0.4, 0.73, and 0.32 in Transects 4-1, 4-2, and 4-6, respectively (Figure 6). During that period of time, NDVI* decreased in Transect 4-2 (due to vegetation clearing in preparation for active restoration) and in Transects 4-3 and 5-2 (Figure 7).

4 | DISCUSSION

4.1 | Changes in vegetation cover and NDVI* after the pulse flow

Vegetation cover along field transects increased in 2015 and NDVI* increased in 2014 (the year of the pulse flow). It is likely that vegetation cover in the transects also increased in 2014, but we do not have ground survey data for 2013 to confirm this. Vegetation cover was highest in 2015, whereas NDVI* did not change during 2014 and 2015, suggesting a lag in the response of vegetation from ground transects to the pulse flow. Lag effects in vegetation response to water deliveries in arid and semiarid systems have been observed in parts of the Tarim River in western China, where the fractional vegetation cover in some portions of the river was correlated to groundwater levels that resulted from river runoff of the previous year (Bao, Huang, Ma, Guo, & Wang, 2017). In the Tarim River, delayed vegetation responses to changes in the groundwater were linked to differences in species drought stress tolerances and differences in soil water content that resulted from texture variations in the soil profile and differences in water deliveries (Tao, Gemmer, Song, & Jiang, 2008). Also, in the study by Tao et al. (2008), vegetation grew more in areas close to the river channel compared with upland areas. Similarly, in the Heihe River Basin in north-western China, time lag responses to runoff varied in different regions. Regions where runoff was lower showed higher time lag responses, as well as the timing in runoff had different effects, along with spring flows that favoured germination versus autumn flows that favoured growth during the next year (Zhang, Ye, Chen, & Zu, 2017). In our study, most of the pulse flow infiltrated into the regional aquifer by the end of the 2014 growing season (Kennedy et al., 2017). However, the vegetation response along ground transects indicates that the soil retained enough water to support vegetation growth for two growing seasons, at least in areas close to the channel. Additional water deliveries in 2015 through Morelos dam and the km 27 spillway (Reach 3) likely also had an effect.

Jarchow et al. (2017) quantified the NDVI* response to the pulse flow by reach including all the pixels within and outside of the inundation zone. At the riparian corridor scale, the green up measured as NDVI* was similar or higher than 2014 in 2015 in Reaches 2 and 4. We observed the same trend in NDVI* in transects from Reach 2, which can be associated to the 2015 water deliveries. In perennial reaches (Reach 1 and Reach 4), our data indicate that the sites are very dynamic and have a high variation in NDVI* during the growing season (Figure 8). This makes difficult to differentiate any responses to the pulse flow from responses that result from variations in irrigation return flows. Moreover, it is also possible that the mismatch between ground surveys and NDVI* in perennial transects could result from variations in plant cover that we did not capture by sampling one time at the end of the growing season. For instance, in some transects from Reach 4, the peak NDVI* was observed in August (Figure 8). This could be resulting from annual vegetation that had died by the end of the growing season or as a result of water level changes that create bare ground for plant establishment for short periods of time.

At the riparian corridor scale, responses in NDVI* are also affected by the vegetation density. In the Tarim River in China, a low variation in NDVI in response to water deliveries was observed in areas with low vegetation cover (Sun, Chang, Opp, & Hennig, 2011). We observed the same pattern in the ephemeral and driest reach (Reach 3), where variations in both cover and NDVI* were small.

Previous studies in the Colorado River Delta riparian corridor indicated vegetation cover estimated through NDVI can increase in response to flow releases. From 1993 to 1999, a series of flows during the winter and spring that varied in peak discharge rates of

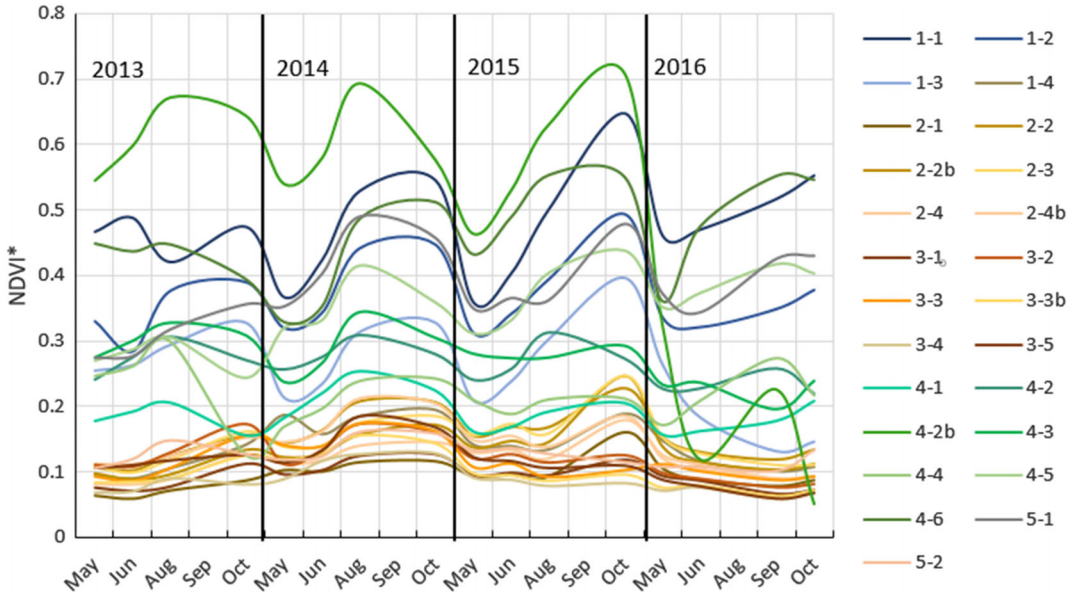


FIGURE 8 NDVI* through the growing season by transect, transect indicated as b, represent side channels. NDVI, normalized difference vegetation index

>500 m^3/s in 1993 to <100 m^3/s during 1997 and >200 m^3/s in the next 2 years were related to increases in vegetation cover of almost 10% that occurred after 3 years of consecutive floods (Zamora-Arroyo & Nagler et al., 2001). This was also supported by Nagler et al. (2005) and Nagler, Glenn, and Hinojosa-Huerta (2009). In comparison, after the 2014 pulse flow, mean vegetation cover in the 21 transects increased 14% (from 33.1% to 47.2%), but the growth was not maintained after the 2015 growing season and vegetation cover returned to 2014 or lower values in most transects of the three first reaches. In 2016, cover in half of the transects in Reaches 4 and 5 was slightly higher (8–16%) compared with 2014 values. This could be associated with the effects of subsequent flows targeted to restoration areas close to the transects location and the high water table documented in Reaches 4 and 5 (Ramírez-Hernández et al., 2015).

Both studies from Nagler et al. (2005, 2009) highlight the link between the 1993 high flow (almost 4 times higher than the 2014 pulse flow) and recruitment of native trees in the corridor. The 2014 pulse flow, by contrast, resulted in minimal establishment of native trees (Shafroth et al., 2017) and a temporary increase in the number of species and vegetation cover.

4.2 | Changes in vegetation composition, structure and NDVI* responses in transects

In our study, the greatest increases in vegetation cover in 2014 and 2015 resulted from species with rapid growth strategies under conditions of soil saturation (*A. donax*, *P. australis*, *T. domingensis*; Vivian, Godfree, Colloff, Mayence, & Marshall, 2014) and herbaceous species classified as facultative and obligate wetland species (*Pluchea odorata*, *Xanthium strumarium*, and *Bacopa monnieri*). *P. sericea* increased almost in all the transects where it was present, and *Tamarix* spp. showed greater increases in cover in transects outside of Reach 3 (the driest section of the river), where groundwater conditions were more favourable. Change in cover of native phreatophytic trees (*S. gooddingii* and *P. fremontii*) was negligible. Native tree cover was <10% in all the transects, which made it difficult to detect any increases that could have indicated a response in growth to the pulse flow. Thus, other methods such as tree ring growth and biomass allocation metrics (height, branches length, and canopy closure) might be more appropriate to evaluate responses in the case of the native trees.

In most cases, changes in vegetation cover can be attributed to foliar cover and vegetative growth versus recruitment of new individuals. Vegetative growth responses, particularly in the clonal shrub *P. sericea* can be expected by early spring floods (Mortenson, Weisberg, & Stevens, 2012). During a related study, we monitored recruitment of *P. fremontii*, *S. gooddingii*, *Baccharis* spp., and *Tamarix* spp. and observed minimal new seedling establishment (Shafroth et al., 2017).

Changes in the NDVI* metric tended to be smaller compared with vegetation cover and sometimes did not match the trends in cover in the transects. This may be due to differences in the extent of surveyed area from ground surveys versus NDVI* polygons. For NDVI*, we surveyed the area of two Landsat pixels (30 m) along each side of the transect; therefore, our transect data will match the Landsat data under the assumption that the vegetation spatial patterns in polygons are homogenous. If there is a high variation on vegetation spatial patterns, we could be capturing spectral signatures from litter, soil wetness, shadows, areas with burned soil, and plant species with higher leaf reflectance, lower light interception values, and lower NDVI values for arrowweed and saltcedar when compared with cottonwood and willow species in natural stands (Nagler et al., 2004). Despite the efforts to reduce noise effects in NDVI datasets through atmospheric corrections and protocols to document and reduce error,

NDVI-derived metrics will contain a degree of noise that tends to impact NDVI values, usually reducing them (Pettorelli et al., 2005). Also, metrics as NDVI do not necessary quantify the vegetation content of the sampled pixel including the vertical structure, because they are capturing the reflectance of the canopy including the different colour background soils; in contrast, vegetation cover from ground surveys included all the overlapping layers of species cover and does not account for this background.

The dissimilarity index indicates that changes in community composition and structure tended to be higher in perennial transects. The highest responses observed in some transects resulted from decreases in the number of species or the relative cover from 1 year to another; however, overall transects presented small changes (≤0.20) for this metric. The utility of this metric to assess responses to environmental flows remains in question because it can be responsive to both increases and decreases in the species presence and cover, without providing information on changes on the target species (native trees). The dissimilarity values or distances between communities need to be linked to differences in ecological functions to become useful for site managers. As Bauer, Harzer, Strobl, and Kollmann (2018) recommended, that in order to evaluate responses to restoration, a focus on functional groups of interest can be more useful than indices that quantify responses in diversity.

4.3 | Recommendations for evaluating vegetation responses to flows

Higher variation in vegetation cover in perennial transects versus lower variation in ephemeral transects is explained by the presence of the functional plant types that respond rapidly to changes in water level. Transects were perpendicular to the river channel and crossed the active channel. Thus, a considerable percentage of the transect in perennial transects is capturing variations in plant cover associated with emergent species (e.g., reeds and cattail). This suggests that the location and orientation of transects/polygons for NDVI* sampling needs to be considered carefully, because this can affect the representativeness and limit interpretations of a more general pattern occurring in the upland habitats. To avoid the inclusion of NDVI contribution from emergent vegetation, we suggest to sample vegetation excluding the channel with surface water if possible. Studies that measured changes in NDVI* at the riparian corridor scale in the delta indicate mostly areas within the inundation zone continued to green up after 2014 (Jarchow et al., 2017; Nagler et al., 2018).

On the other hand, our sampling design can be very useful for detecting the effects of groundwater variation on streambed vegetation and adjacent locations. For example, in Transect 1-3, an important drop in NDVI* and vegetation cover occurred in 2016. The NDVI* drop was likely a result of decreased groundwater levels. In this transect, we did not observe surface water in the channel in 2016 (which we had in previous years), and patches mainly composed of emergent species desiccated. Groundwater levels in Reach 2 and 3 were affected by a cone of depression (areas where the water table drops) as a result of groundwater over pumping (Kennedy et al., 2017). The expansion of the depressed ground water levels into the south portion of Reach 1 could be causing the changes in the extent of the surface water in the streambed (International Boundary and Water Commission, 2018). Changes in groundwater in turn can also alter the composition and structure of plant communities. This suggests that the continuous monitoring of NDVI* responses in the perennial portions of the riparian corridor could be very useful for detecting changes in vegetation cover that result from changes in the groundwater table as well as for differentiating permanent changes in vegetation cover from other events such as small fires. Other approaches can include analysis of spatial and temporal variability of NDVI* and other vegetation indices in response to water deliveries at the pixel scale (Jarchow et al., 2017; Shanafield et al., 2017; Sun et al., 2011).

A correlation between vegetation cover and NDVI from different sensors has been explored by several authors (Carlson & Ripley, 1997; Duncan, Stow, Franklin, & Hope, 1993; Nagler et al., 2001, 2004). This work also pointed to similar strong correlation every year of the study supporting findings by Nagler et al. (2001), who estimated 84% of variation in cover associated with NDVI, compared with a range of 84–88% in the present study. Our study also indicates that the strength of the relationship is not altered by the method used to estimate ground cover, because we used a line intercept method versus aerial cover estimations in plots.

The relationship between NDVI from Landsat and vegetation cover could be useful to detect trends in vegetation cover at the riparian corridor scale, but it does not provide information on the species causing the trends. The dominant species (*Tamarix* spp.) and arrowweed (*P. sericea*) have NDVI ranges that can overlap (0.3–0.8 and 0.1–0.4, respectively; Nagler et al., 2001, 2004). Moreover, target native tree species (*P. fremontii* and *S. gooddingii*) with a NDVI range of 0.4–0.8 overlaps with the saltcedar NDVI range (Nagler et al., 2001, 2004). Other approaches like phenology of species should be explored if the goal is to extract information on species cover using satellite images. Another possibility to extract information on species composition to explain NDVI trends is to incorporate a high-resolution aerial photography collected with unmanned aerial system and to explore other spectral indices or properties of the target species. Lastly, the analysis of landscape metrics such as riparian vegetation patches dimension, number, and distribution, along with textural and spectral metrics extracted from high-resolution images can be used in riparian systems to track changes in vegetation structure and composition at the landscape scale (Aguiar, Fernandes, & Ferreira, 2011; Fernandes, Aguiar, Silva, Ferreira, & Pereira, 2014).

5 | CONCLUSIONS

Greenness measured through satellite NDVI* increased 15% in 2014, and vegetation cover increased 14% in 2015; both returned to pre-pulse (2013) conditions in 2016. Similarly, changes in vegetation structure and composition were also temporary, as vegetation

communities returned to previous conditions, suggesting that one pulse of water in the spring of 1 year, but none in following years, was not enough to sustain growth for the 2 years following the 2014 pulse year observed in this study. Increases in vegetation cover in 2014 or 2015 resulted mainly from plants with rapid growth strategies, such as reeds, cattail, herbaceous species, and vegetative growth. The greatest increases in the dominant *Tamarix* spp. cover were outside of Reach 3, in reaches where groundwater conditions are favourable. *P. sericea*, a clonal native shrub, was very responsive to the pulse flow. Native trees presented low increases in cover (1%) that were difficult to assess due their low presence in the riparian corridor. To assess responses to flows in these species would require including different approaches that can quantify growth through analysis of tree ring patterns, tree height, diameter, and metrics that can detect changes in biomass allocation.

The strong relationship and consistency in the association between NDVI* and vegetation cover highlight the relevance of continued monitoring of the riparian corridor using designs that (a) characterize the NDVI spatiotemporal dynamics in response to water deliveries, (b) detect changes in plant communities that can be resulting from alterations in the groundwater conditions and other events, and (c) are complemented with high-resolution imagery or ground data the helps to identify which species are contributing to the observed NDVI trend.

This study shows that incorporating ground surveys (or other methods such as drones) that provide community composition and structure, in conjunction with recruitment data, can supplement characterizations of vegetation growth or green-up responses to environmental flows rather than using NDVI alone.

ACKNOWLEDGEMENTS

This manuscript started under the mentorship of the late Dr. Edward P. Glenn. We thank him for his dedication towards the restoration of the Colorado River Delta ecosystems and for sharing his enthusiasm, knowledge, and ideas with the ones that had the privilege to work closely with him. We thank Erick Lundgren (Arizona State University), Alejandra Calvo-Fonseca, and Juan Butrón Méndez (Pronatura A.C.) for their work collecting the data for the vegetation surveys. We also acknowledge the Minute 319 Science Team for their contributions on numerous aspects of the Minute 319 project research and monitoring activities. Funding for M. M. G.-S., K. W. F., and E. P. W. was provided by the Department of Interior, Bureau of Reclamation, and International Boundary and Water Commission. Funding for C. J. J., P. B. S., and P. L. N. was provided by the U.S. Geological Survey. We also thank the International Boundary and Water Commission (IBWC) and Comisión Internacional de Límites y Aguas for their logistic support. Any use of trade, firm, or product names is for descriptive purposes only and does not imply endorsement by the U.S. Government.

AUTHOR CONTRIBUTIONS

M.M.G.-S. and C.J.J. conceived the research idea to use ground and remotely sensed research for this study. C.J.J. collected the imagery. K.F. provided funding and leadership. P.S. provided the ground-based protocol. E.P.G., C.J.J., and P.L.N. provided advice on acquiring and analysing the remote sensing component. E.P.G. assisted with research design. M.M.G.-S., C.J.J., P.B.S., and P.L.N. wrote and edited the manuscript.

DATA AVAILABILITY STATEMENT

Data available on request from the authors

ORCID

Martha M. Gómez-Sapiens https://orcid.org/0000-0002-4839-5924
Christopher J. Jarchow https://orcid.org/0000-0002-0424-4104
Patrick B. Shafroth https://orcid.org/0000-0002-6064-871X

REFERENCES

Acreman, M. C., Overton, I. C., King, J., Wood, P., Cowx, I. G., Dunbar, M. J., … Young, W. (2014). The changing role of eco-hydrological science in guiding environmental flows. *Hydrological Sciences Journal*, *59*(3–4), 433–450. https://doi.org/10.1080/02626667.2014.886019

Aguiar, F. C., Fernandes, M. R., & Ferreira, M. T. (2011). Riparian vegetation metrics as tools for guiding ecological restoration in riverscapes. *Knowledge and Management of Aquatic Ecosystems*, *402*, 21. http://doi.org/10.1051/kmae/2011074

Auble, G. T., Friedman, J. M., & Scott, M. L. (1994). Relating riparian vegetation to present and future streamflows. *Ecological Applications*, *4*(3), 544–554. https://doi.org/10.2307/1941956

Bao, A., Huang, Y., Ma, Y., Guo, H., & Wang, Y. (2017). Assessing the effect of EWDP on vegetation restoration by remote sensing in the lower reaches of Tarim River. *Ecological Indicators*, *74*, 261–275. https://doi.org/10.1016/j.ecolind.2016.11.007

Bauer, M., Harzer, R., Strobl, K., & Kollmann, J. (2018). Resilience of riparian vegetation after restoration measure on river inn. *River Research Applications*, *34*, 451–460. http://doi.org/10.1002.rra.3255

Bland, J. M., & Altman, D. G. (1995). Multiple significance tests: The Bonferroni method. *BMJ*, *310*(6973), 170. https://doi.org/10.1136/bmj.310.6973.170

Bray, J. R., & Curtis, J. T. (1957). An ordination of upland forest communities of southern Wisconsin. *Ecological Monographs*, *27*(4), 325–349. http://doi.org/10.2307/1942268

Busch, D. E., & Smith, S. D. (1995). Mechanisms associated with decline of woody species in riparian ecosystems of the southwestern U.S. *Ecological Monographs*, *65*(3), 347–370.

Canfield, R. H. (1941). Application of the line interception method in sampling range vegetation. *Journal of Forestry*, *39*(4), 388–394. https://doi.org/10.1093/jof/39.4.388

Carlisle, D. M., Wolock, D. M., & Meador, M. R. (2011). Alteration of streamflow magnitudes and potential ecological consequences: A multiregional assessment. *Frontiers in Ecology and the Environment*, *9*(5), 264–270. https://doi.org/10.1890/100053

Carlson, T. N., & Ripley, D. A. (1997). On the relation between NDVI, fractional vegetation cover. *And Leaf Area Index, Remote Sensing of Environment*, *62*(3), 241–252. http://doi.org/10.1016/s0034-4257(97)00104-1

Cohen, M. J., Henges-Jeck, C., & Castillo-Moreno, G. (2001). A preliminary water balance for the Colorado River Delta, 1992-1998. *Journal of Arid Environments*, *49*(1), 35–48. https://doi.org/10.1006/jare.2001.0834

Duncan, J., Stow, D., Franklin, J., & Hope, A. (1993). Assessing the relationship between spectral vegetation indices and shrub cover in the Jornada Basin, New Mexico. *International Journal of Remote Sensing*, *14*(18), 3395–3416.

Fernandes, M. R., Aguiar, F. C., Silva, J. M. N., Ferreira, M. R., & Pereira, J. M. C. (2014). Optimal attributes for the object based detection of giant reed in riparian hábitats: A comparative study between airborne high spatial resolution and WorldView-2 imagery. *International Journal of Applied Earth Observation and Geoinformation*, *32*, 79–91.

Flessa, K. W., Glenn, E. P., Hinojosa-Huerta, O., De la Parra-Renteria, C. A., Ramírez-Hernández, J., Schmidt, J. C., & Zamora-Arroyo, F. A. (2013). Flooding the Colorado River Delta: A landscape-scale experiment. *EOS American Geophysics Union*, *94*(50), 11–486. https://doi.org/10.1002/2013EO500001

Friedman, J., Osterkamp, W., & Lewis, W. (1996). Channel narrowing and vegetation development following a Great Plains Flood. *Ecology*, *77*(7), 2167–2181. http://doi.org/10.2307/2265710

Glenn, E. P., Flessa, K. W., Kendy, E., Shafroth, P. B., Ramírez-Hernández, J., Gomez-Sapiens, M., & Nagler, P. L. (2017). Environmental flows for the Colorado River Delta: Results of an experimental pulse flow release from the US to Mexico. *Ecological Engineering*, *106*(Part B).

Glenn, E. P., Huete, A. R., Nagler, P. L., Hirschboeck, K. K., & Brown, P. (2007). Integrating remote sensing and ground methods to estimate evapotranspiration. *Critical Reviews in Plant Sciences*, *26*(3), 139–168.

Glenn, E. P., Huete, A. R., Nagler, P. L., & Nelson, S. G. (2008). Relationship between remotely-sensed vegetation indices, canopy attributes and plant physiological processes: What vegetation indices can and cannot tell us about the landscape. *Sensors*, *8*(4), 2136–2160. https://doi.org/10.3390/s8042136

Glenn, E. P., Nagler, P. L., & Huete, A. R. (2014). Change detection using vegetation indices and multiplatform satellite imagery at multiple temporal and spatial scales. In Q. Weng (Ed.), *Scale issues in remote sensing* (pp. 79–107). New Jersey, USA: John Wiley & Sons, Inc.

González, E., Sher, A. A., Tabacchi, E., Masip, A., & Poulin, M. (2015). Restoration of riparian vegetation: A global review of implementation and evaluation approaches in the international, peer-reviewed literature. *Journal of Environmental Management*, *158*, 85–94. http://doi.org/10.1016/j.jenvman.2015.04.033

Groeneveld, D. P., & Baugh, W. M. (2007). Correcting satellite data to detect vegetation signal for eco-hydrologic analysis. *Journal of Hydrology*, *344*(1–2), 135–145. https://doi.org/10.1016/j.jhydrol.2007.07.001

Hinojosa-Huerta, O., Nagler, P. L., Carrillo-Guerrero, Y. K., & Glenn, E. P. (2013). Effects of drought on birds and riparian vegetation in the Colorado River Delta, Mexico. *Ecological Engineering*, *51*, 275–281. https://doi.org/10.1016/j.ecoleng.2012.12.082

IBM Corp., (2016). IBM SPSS Statistics for Windows, Version 24.0. Armonk, NY: IBM Corp. R Core Team. 2017. R: A language and environment for statistical computing. R Foundation for Statistical Computing, Vienna, Austria.

International Boundary and Water Commission, 2018. Minute 319 Colorado River Limitrophe and Delta Environmental Flows Monitoring Final Report, November 28, 2018.

International Boundary and Water Commission, 2012. Minute No. 319-Interim International Cooperative Measures in the Colorado River Basin Through 2017 and Extension of Minute 318 Cooperative Measures to Address the Continued Effects of the April 2010 Earthquake in the Mexico Valley, Baja California. International Boundary Water Commission.

Jarchow, C. J., Nagler, P. L., & Glenn, E. P. (2017). Greenup and evapotranspiration following the Minute 319 pulse flow to Mexico: An analysis using Landsat 8 normalized difference vegetation index (NDVI) data. *Ecological Engineering*, *106*(Part B), 776–783. https://doi.org/10.1016/j.ecoleng.2016.08.007

Jarchow, C. J., Nagler, P. L., Glenn, E. P., Ramírez-Hernández, J., & Rodríguez-Burgueño, J. E. (2017). Evapotranspiration by remote sensing: An analysis of the Colorado River Delta before and after the Minute 319 pulse flow. *Ecological Engineering*, *106*(Part B), 725–732. https://doi.org/10.1016/j.ecoleng.2016.10.056

Jensen, J. R. (1981). Urban change detection mapping using Landsat digital data. *The American Cartographer*, *8*(2), 127–147. https://doi.org/10.1559/152304081784447318

Jiang, Z. and Huete, A. (2010). Linearization ofNDVI based on its relationship with vegetation fraction. *Photogrammetric Engineering & Remote Sensing*, *76*(8), 965–975. http://doi.org/10.14358/PERS.76.8.965

Jones, B. K., Edmonds, C. E., Slonecker, E. T., Wickham, J. D., Neale, A. C., & Wade, T. G. (2008). Detecting changes in riparian habitat conditions based on patterns of greenness change: A case study from the Upper San Pedro River basin, USA. *Ecological Indicators*, *8*, 89–99.

Kennedy, J., Rodríguez-Burgueño, J. E., & Ramírez-Hernández, J. (2017). Groundwater response to the 2014 pulse flow in the Colorado River Delta. *Ecological Engineering*, *106*(Part B), 715–724. https://doi.org/10.1016/j.ecoleng.2016.10.072

Mortenson, S. G., Weisberg, P. J., & Stevens, L. E. (2012). The influence of floods and precipitation on *Tamarix* establishment in Grand Canyon, Arizona: Consequences for flow regime restoration. *Biological Invasions*, *14*(5), 1061–1076. http://doi.org/10.1007/s10530-011-0139-z

Mueller, E. R., Schmidt, J. C., Topping, D. J., Shafroth, P. B., Rodríguez-Burgueño, J. E., Hernández-Ramírez, J., & Grams, P. E. (2017). Geomorphic change and sediment transport during a small artificial flood in a transformed post-dam delta: The Colorado River Delta, United States and Mexico. *Ecological Engineering*, *106*(Part B), 757–775. https://doi.org/10.1016/j.ecoleng.2016.08.009

Nagler, P. L., Glenn, E. P., & Hinojosa-Huerta, O. (2009). Synthesis of ground and remote sensing data for monitoring ecosystem functions in the Colorado River Delta, Mexico. *Remote Sensing of Environment*, *113*(7), 1473–1485. https://doi.org/10.1016/j.rse.2008.06.018

Nagler, P. L., Glenn, E. P., & Huete, A. R. (2001). Assessment of spectral vegetation indices for riparian vegetation in the Colorado River Delta, Mexico. *Journal of Arid Environments*, *49*(1), 91–110. https://doi.org/10.1006/jare.2001.0844

Nagler, P. L., Glenn, E. P., Thompson, T. L., & Huete, A. R. (2004). Leaf area index and normalized vegetation difference index as predictors of canopy characteristics and light interception by riparian species on the lower Colorado River. *Agricultural and Forest Meteorology*, *125*(1–2), 1–17. https://doi.org/10.1016/j.agrformet.2004.03.008

Nagler, P. L., Hinojosa-Huerta, O., Glenn, E. P., Garcia-Hernandez, J., Romo, R., Curtis, C., … Nelson, S. (2005). Regeneration of native trees in the presence of saltcedar: Results of an inadvertent, 20 year pulse-flood experiment in the Colorado River Delta, Mexico. *Conservation Biology*, *19*(6), 1842–1852. https://doi.org/10.1111/j.1523-1739.2005.00234.x

Nagler, P. L., Jarchow, C. J., & Glenn, E. P. (2018). Remote sensing vegetation index methods to evaluate changes in greenness and evapotranspiration in riparian vegetation in response to the Minute 319 environmental pulse flow to Mexico. *Proceedings of the International Association of Hydrological Sciences*, *95*, 1–10. https://doi.org/10.5194/piahs-380-45-2018

Naiman, R., Decamps, H., & Pollock, M. (1993). The role of riparian corridors in maintaining regional biodiversity. *Ecological Applications*, *3*(2), 209–212. http://doi.org/10.2307/1941822

Naiman, R. J., & Decamps, H. (1997). The ecology of interfaces: Riparian zones. *Annual Review of Ecology and Systematics*, *28*, 621–658. https://doi.org/10.1146/annurev.ecolsys.28.1.621

Nguyen, U., Glenn, E. P., Nagler, P. L., & Scott, R. L. (2015). Long-term decrease in satellite vegetation indices in response to environmental variables in an iconic desert riparian ecosystem: The Upper San Pedro, Arizona, United States. *Ecohydrology*, *8*(4), 610–625. https://doi.org/10.1002/eco.1529

Nilsson, C., & Berggren, K. (2000). Alterations of riparian ecosystems caused by river regulation dam operations have caused global-scale ecological changes in riparian ecosystems. How to protect river environments and human needs of rivers remains one of the most

important questions of our time. *Bioscience*, *50*(9), 783–792. https://doi.org/10.1641/0006-3568(2000)050[0783:AORECB]2.0.CO;2

Pettorelli, N., Vik, J. O., Mysterud, A., Gaillard, J.-M., Tucker, C. J., & Stenseth, N. C. (2005). Using the satellite-derived NDVI to assess ecological responses to environmental change. *Trends in Ecology & Evolution*, *20*(9), 503–510. https://doi.org/10.1016/j.tree.2005.05.011

Pitt, J., & Kendy, E. (2017). Shaping the 2014 Colorado River Delta pulse flow: Rapid environmental flow design for ecological outcomes and scientific learning. *Ecological Engineering*, *106*(Part B), 704–714. http://doi.org/10.1016/j.ecoleng.2016.12.002

Poff, N. L., Allan, K. D., Bain, M. B., Karr, J. R., Prestegaard, K. L., Richter, B. D., … Stromberg, J. C. (1997). The natural flow regime: A paradigm for river conservation and restoration. *BioScience*, *47*(11), 769–784. http://doi.org/10.2307/1313099

Poff, N. L., Koestner, K. A., Neary, D. G., & Henderson, V. (2011). Threats to riparian ecosystems in Western North America: An analysis of existing literature. *Journal of the American Water Resources Association*, *47*(6), 1241–1254. https://doi.org/10.1111/j.1752-1688.2011.00571.x

Ramírez-Hernández, J., Hinojosa-Huerta, O., Peregrina-Llanes, M., Calvo-Fonseca, A., & Carrera-Villa, E. (2013). Groundwater responses to controlled water releases in the limitrophe region of the Colorado River: Implications for management and restoration. *Ecological Engineering*, *59*, 111–120. https://doi.org/10.1016/j.ecoleng.2013.02.016

Ramírez-Hernández, J., Rodríguez-Burgueño, J. E., Kendy, E., Salcedo-Peredia, A., & Lomelí, M. A. (2017). Hydrological response to an environmental flood: Pulse flow 2014 on the Colorado River Delta. *Ecological Engineering*, *106*(Part B), 633–644.

Ramírez-Hernández, J., Rodriguez-Burgueño, J. E., Zamora-Arroyo, F., Carreon-Diazconti, C., & Perez-Gonzalez, D. (2015). Mimic pulse-base flows and groundwater in a regulated river in semiarid land: Riparian restoration issues. *Ecological Engineering*, *83*, 239–248. https://doi.org/10.1016/j.ecoleng.2015.06.006

Richardson, D. M., Holmes, P. M., Esler, K. J., Galatowitsch, S. M., Stromberg, J. C., Kirkman, S. P., … Hobbs, R. J. (2007). Riparian vegetation: Degradation, alien plant invasions, and restoration prospects. *Diversity and Distributions*, *13*(1), 126–139. https://doi.org/10.1111/j.1366-9516.2006.00314.x

Ricotta, C., & Podani, J. (2017). On some properties of the Bray-Curtis dissimilarity and their ecological meaning. *Ecological Complexity*, *31*, 201–205. https://doi.org/10.1016/j.ecocom.2017.07.003.

Sankey, J. B., Ralston, B. E., Grams, P. E., Schmidt, J. C., & Cagney, L. E. (2015). Riparian vegetation, Colorado River, and climate: Five decades of spatiotemporal dynamics in the Grand Canyon with river regulation. *Journal of Geophysical Research: Biogeosciences*, *120*(8), 1532–1547. https://doi.org/10.1002/2015JG002991

Shafroth, P. B., Auble, G. T., Stromberg, J. C., & Patten, D. T. (1998). Establishment of woody riparian vegetation in relation to annual patterns of streamflow, Bill Williams River, Arizona. *Wetlands*, *18*(4), 577–590. https://doi.org/10.1007/BF03161674

Shafroth, P. B., Schlatter, K. J., Gomez-Sapiens, M., Lundgren, E., Grabau, M. R., Ramírez-Hernández, J., … Flessa, K. W. (2017). A large-scale environmental flow experiment for riparian restoration in the Colorado River Delta. *Ecological Engineering*, *106*(Part B), 633–644 http//doi.org/10.1016/j.ecoleng.2017.02.016.

Shanafield, M., Gutierrez-Jurado, H., Rodríguez-Burgueño, J. E., Ramírez-Hernández, J., Jarchow, C., & Nagler, P. L. (2017). Short-term and long-term evapotranspiration rates at ecological restoration sites along a large river receiving rare flow events. *Hydrological Processes*, *31*(24), 4328–4337. https://doi.org/10.1002/hyp.11359

Sprenger, M. D., Smith, L. M., & Taylor, J. P. (2002). Restoration of riparian habitat using experimental flooding. *Wetlands*, *22*(1), 49–57. https://doi.org/10.1672/0277-5212(2002)022[0049:RORHUE]2.0.CO;2

Stevens, L. E., Ayers, T. J., Bennett, J. B., Christensen, K., Kearsley, M. J. C., Meretsky, V. J., … Wegner, D. L. (2001). Planned flooding and Colorado River riparian trade-offs downstream from Glenn Canyon Dam, Arizona. *Ecological Applications*, *11*(3), 701–710. http://doi.org/10.2307/3061111

Storey, J., Roy, D. P., Masek, J., Gascon, F., Dwyer, J., Choate, M. (2016). A note on the temporary misregistration of Landsat-8 Operational Land Imager (OLI) and Sentinel-2 Multi Spectral Instrument (MSI) Imagery. *Remote Sensing of Environment*, *186*(1), 121–122. http://doi.org/10.1016/j.rse.2016.08.025

Stromberg, J. C. (1998). Dynamics of Fremont cottonwood (*Populus fremontii*) and saltcedar (*Tamarix chinensis*) populations along the San Pedro River. *Arizona. Journal of Arid Environments*, *40*(2), 133–155. https://doi.org/10.1006/jare.1998.0438

Sun, Z., Chang, N., Opp, C., & Hennig, T. (2011). Evaluation of ecological restoration through vegetation patterns in the lower Tarim river, China with MODIS NDVI data. *Ecological Informatics*, *6*(2), 156–163. https://doi.org/10.1016/j.ecoinf.2010.10.002

Tao, H., Gemmer, M., Song, Y., & Jiang, T. (2008). Ecohydrological responses on water diversion in the lower reaches of the Tarim River, China. *Water Resources Research*, *44*(8), W08422.

Vermote, E., Justice, C., Claverie, M., & Franch, B. (2016). Preliminary analysis of the performance of the Landsat 8/OLI land surface reflectance product. *Remote Sensing of Environment*, *185*, 46–56. http://doi.org/10.1016/j.rse.2016.04.008.

Vivian, L. M., Godfree, R. C., Colloff, M. J., Mayence, C. E., & Marshall, D. J. (2014). Wetland plant growth under contrasting water regimes associated with river regulation and drought: Implications for environmental water management. *Plant Ecology*, *215*(9), 997–1011. https://dx.doi.org/10.1007/s11258-014-0357-4

Zamora-Arroyo, F., Nagler, P. L., Briggs, M., Radtke, D., Rodriguez, H., Garcia, J., … Glenn, E. P. (2001). Regeneration of native trees in response to flood releases from the United States into the delta of the Colorado River, Mexico. *Journal of Arid Environments*, *49*(1), 49–64. https://doi.org/10.1006/jare.2001.0835

Zhang, S., Ye, Z., Chen, Y., & Xu, Y. (2017). Vegetation responses to an ecological water conveyance project in the lower reaches of the Heihe River basin. *Ecohydrology*, *10*(6), 10, e1866. http://doi.org/10.1002/eco.1866

Zhao, Y., Wei, Y., Li, S., & Wu, B. (2016). Downstream ecosystem responses to middle reach regulation of river discharge in the Heihe River Basin, China. *Hydrology and Earth Systems Science*, *20*(11), 4469–4481. https://doi.org/10.5194/hess-20-4469-2016

How to cite this article: Gómez-Sapiens MM, Jarchow CJ, Flessa KW, Shafroth PB, Glenn EP, Nagler PL. Effect of an environmental flow on vegetation growth and health using ground and remote sensing metrics. *Hydrological Processes*. 2020;34:1682–1696. https://doi.org/10.1002/hyp.13689